Available online at www.sciencedirect.com
ScienceDirect
Progress in Natural Science 18 (2008) 1465–1473
Progress in Natural Science
www.elsevier.com/locate/pnsc

Review

Progress in modeling of fluid flows in crystal growth processes

Qisheng Chen *, Yanni Jiang, Junyi Yan, Ming Qin

Institute of Mechanics, Chinese Academy of Sciences, Beijing 100190, China

Received 3 March 2008; received in revised form 6 June 2008; accepted 10 June 2008

Abstract

Modeling of fluid flows in crystal growth processes has become an important research area in theoretical and applied mechanics. Most crystal growth processes involve fluid flows, such as flows in the melt, solution or vapor. Theoretical modeling has played an important role in developing technologies used for growing semiconductor crystals for high performance electronic and optoelectronic devices. The application of devices requires large diameter crystals with a high degree of crystallographic perfection, low defect density and uniform dopant distribution. In this article, the flow models developed in modeling of the crystal growth processes such as Czochralski, ammonothermal and physical vapor transport methods are reviewed. In the Czochralski growth modeling, the flow models for thermocapillary flow, turbulent flow and MHD flow have been developed. In the ammonothermal growth modeling, the buoyancy and porous media flow models have been developed based on a single-domain and continuum approach for the composite fluid-porous layer systems. In the physical vapor transport growth modeling, the Stefan flow model has been proposed based on the flow-kinetics theory for the vapor growth. In addition, perspectives for future studies on crystal growth modeling are proposed.

Keywords: Modeling; Crystal growth; Fluid flow; Czochralski growth; Ammonothermal growth; Physical vapor transport

1. Introduction

Most bulk crystals are grown from melt [1], solution [2] or vapor [3], where solutal or/and thermal gradients exist. Czochralski crystal growth method has been the main production method due to its large diameter growth capacities, while solution growth technique has been used for the production of quartz and other oxides, and vapor growth technique has been used for the production of wide-bandgap crystals. In what follows, we will introduce the three methods for crystal growth, the Czochralski method, the ammonothermal method and the vapor growth method.

1.1. Czochralski method

Czochralski method has a history of more than ninety years since Czochralski used it to pull single crystalline wires of low melting point metals from melt [4], and it is now the most dominant method for growing silicon crystals which are the most important material for the electronic industry. Fig. 1 shows the schematic diagram of the growth process in a typical silicon growth furnace used by industries. The melt flow inside the crucible is complicated due to buoyancy, surface tension, centrifugal and Lorentz forces.

1.2. Ammonothermal growth

For the ammonothermal growth, aqueous ammonia is used as a solvent under high temperatures and high pressures to dissolve and recrystallize materials that are relatively insoluble under ordinary conditions. The similarity

* Corresponding author. Tel.: +010 82544092; fax: +010 82544096.
E-mail address: qschen@imech.ac.cn (Q. Chen).

1002-0071/$ - see front matter
doi:10.1016/j.pnsc.2008.06.003

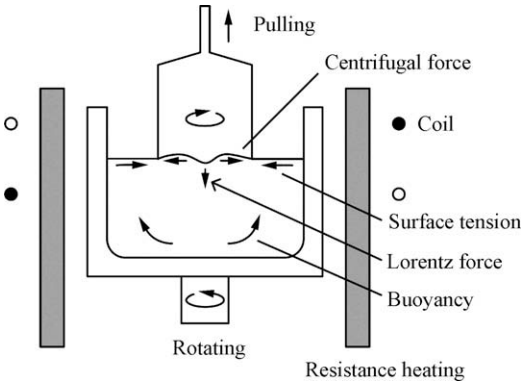

Fig. 1. Schematic diagram of the Czochralski growth process [1].

of ammonia and water as polar solvents allows GaN crystals to grow in ammonia solvents in the same way as the hydrothermal growth of oxides crystals in high-pressure water solutions. GaN is an emerging semiconductor material that could have an enormous impact in the electronics industry. GaN-devices have gained rapid development in the last ten years since the major technological hurdles were overcome in the early 1990s [5]. Fig. 2 shows the convection system for the ammonothermal growth, which consists of a porous bed whose height changes with time, a fluid layer overlying the porous bed, a metal baffle with holes positioned above the porous bed, and solid seed plates whose size increases with the growth. After the ammonothermal system is pressurized, solvent such as ammonia occupies most of the volume.

1.3. Vapor growth

The vapor growth technique has been used for wide-bandgap crystals such as silicon carbide. Silicon carbide is a third-generation semiconductor material which can be used to fabricate electronic and optoelectronic devices that are capable of operating under high-temperature, high-power and high-frequency conditions. Seeded sublimation growth technique (modified Lely method) has been widely used to produce SiC crystals since the 1970s [6]. The bulk growth of SiC by the physical vapor transport (PVT) method involves many important physical phenomena (Fig. 3), such as electromagnetic field, induction heating, conduction and radiation heat transfer, sublimation and condensation, Stefan flow, mass transport, and thermally induced stress.

Since crystal growth experiments are expensive and time-consuming, modeling becomes an effective tool for research and optimization of growth processes. Besides being related to the materials chemistry and physics, the crystal growth technology is more closely linked to fluid dynamics, thermodynamics and heat transfer. During the past thirty years or so, the finite element- or finite volume-based computer aided design (CAD) packages have reached a new height and are now being widely used in industries in designing, manufacturing and final testing of mechanical and thermal systems. Tremendous advancements have also been made in modeling of crystal growth processes. Modeling and simulation of crystal growth processes have reached a point where they can be successfully used to study the basic physical phenomena of the process, to propose modifications in the existing processes and systems, and to design and develop new systems. It is expected that modeling and simulation can greatly reduce the capital investment for the furnace scale-up. Furthermore, the defect density in silicon wafer is strongly related to the thermal history of the growth, the pulling rate and cooling rate. It is desirable to perform simulations of the growth process for a variety of parameters such as pulling rate, rotation speed, and power input.

To meet the next generation technology and application needs, the research, design and development should adopt a system strategy in which crystal growth technology is developed by designing/redesigning one or more (or all) processing steps of the manufacturing cycle and the

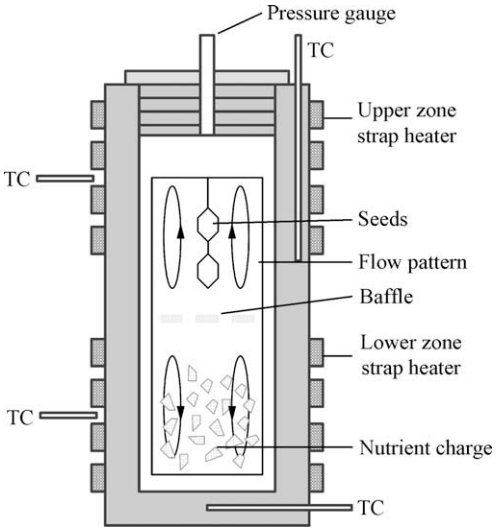

Fig. 2. Schematic diagram of an ammonothermal growth system [2].

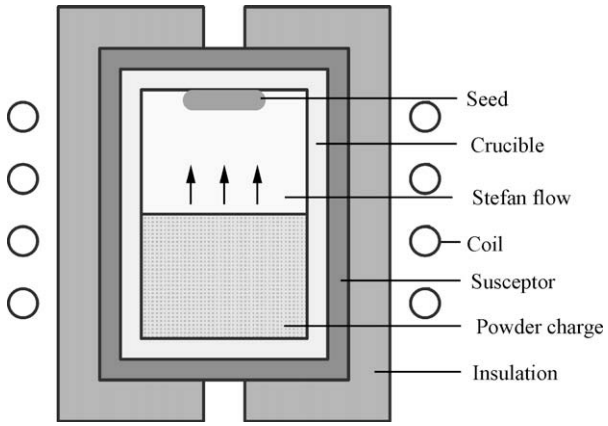

Fig. 3. Schematic diagram of an RF heated furnace for the growth of single SiC crystals by PVT [3].

associated equipment in the shortest possible cycle time. For example, if crystals of a special material are needed, one can start with the materials chemistry and physics, and follow a complete path of process design and development: modeling, simulation and design (virtual growth), model experiments and process optimization, real growth for a range of optimized conditions, and growth system modification or redesign if necessary. The model developed can account for various kinds of physical phenomena including buoyancy, surface tension and centrifugal forces, flow oscillations and turbulence, transport of dopant and impurity species (e.g. Fickian and Soret), segregation, spectral (wavelength-dependent) radiation exchange, volumetric radiation through non-homogeneous, anisotropic media, applied magnetic field, moving and deformable interfaces, and thermal-elastic and visco-plastic stress phenomena.

2. Silicon Czochralski growth modeling

Modeling of the Czochralski growth has attracted tremendous research interests in the last 30 years. Fluid flow is a basic phenomenon in crystal growth processes which results in the formation of macro- and micro-inhomogeneities. The flow model is the most difficult part of modeling, since one has to take into consideration the interactions of different convection mechanisms, e.g. buoyancy, rotation and thermocapillary flows. Modeling and numerical simulation based on physics have become one of the most important research methods for silicon single crystal growth.

2.1. Thermocapillary flow model

In the early days, researchers only considered conduction-dominated heat transfer in the melt without considering convective heat transfer. Supported by the NASA microgravity sciences program in the 1980s, Derby and Brown [7,8] developed a thermal-capillary model for heat transfer in a Cz system, which accounts for conduction-dominated heat transfer throughout the Cz system and includes calculation of the crystal/melt and melt/gas interfaces. Finite element discretization was used for the temperature field and interface shapes. Brown et al. [9] reviewed a hierarchy of models designed for the analysis of transport processes in Czochralski and liquid-encapsulated Czochralski crystal growth. This coupling between heat transfer and the surface shapes had been demonstrated by analyses based solely on conductive heat transfer in the melt. Bornside et al. [10] added diffuse-gray radiation throughout the system. This approach was called the integrated thermal-capillary model (ITCM) at that time.

2.2. Turbulent flow model

The turbulence models for the melt flows were included later to better predict the heat transfer in the melt. Kinney and Brown [11] extended the integrated hydrodynamic thermal-capillary model (IHTCM) of Czochralski growth for large-diameter silicon crystals to include a k-ε model for turbulence in the melt implemented in a form appropriate for capturing the transition to nearly laminar flow near the solid boundaries. These results predicted the enhancement in the heat and mass transfer seen in experiments with increased crucible rotation rate, which was not predicted by laminar flow simulations. Lipchin and Brown [12] tested k-ε turbulence models for turbulent convection in the calculation of the flow, temperature field and oxygen transport in the Czochralski melt. The three formulations tested are the standard k-ε model using wall functions at solid boundaries, k-ε model with a one-equation model for the flow near solid boundaries, and low-Reynolds number k–ε model that does not require an independent description of the flow near the wall. Lipchin and Brown [13] merged the finite-element method for the solution of the ITCM and the finite-volume method for the calculation of turbulent convection.

Jafri et al. [14] numerically studied the effects of the crucible partition on the melt flow and found that a crucible partition shorter than the melt height can significantly improve the melt conditions. Zhang and Prasad [15] presented finite-volume calculations based on a discretization with a nonorthogonal curvilinear grid. They proposed the governing equations in curvilinear coordinates and transformed the computational domain into a rectangular region. Chui et al. [16] implemented a high-resolution parallel scheme for simulation of the Czochralski crystal growth processes. Zhang et al. [17] used a dynamic model to simulate Cz growth of silicon crystal.

Calculations of the melt flows and oxygen distributions were performed by Zhang et al. [18] for the 200 mm and 300 mm diameter growth under different process conditions. An interactive control algorithm was developed to control the power input, pulling rate and crystal diameter. Using the renormalization group (RNG) k-ε model, the effects of buoyancy and crystal and crucible rotations on the melt flow and heat transfer were studied. They simulated the melt flow and oxygen transport for the 300 mm diameter silicon growth using 600 mm and 750 mm diameter crucibles. In the 750 mm diameter crucible, the Grashof number was up to 7×10^{10} if the temperature between the crucible and the crystal was maintained at 85 K.

Nunes and Naraghi [19] used a radiation model called discrete exchange factor (DEF) to simulate a Cz growth system. The governing equations for the DEF method are obtained by discretizing the integral equations of continuous exchange factor (CEF). Gevelber [20] used a lump model to model the Cz growth system.

Kakimoto et al. [21] studied the flow instability of molten silicon in the Czochralski configuration by in-situ observation of melt convection using X-ray radiography and by temperature fluctuation measurement during the crystal growth. The flow instability area, which was also thermally unstable, was found to be larger in the crystal/

crucible iso-rotation condition. Kakimoto et al. [22] numerically simulated fluid flow, heat conduction and heat exchange by radiation using the geometry of a real Czochralski furnace for silicon single crystal growth. The calculated flow velocity and particle path are semi-quantitatively identical to the results obtained from X-ray radiography experiment. Assaker et al. [23] simulated the dynamics of the growth of a 40 cm silicon crystal. The effect of melt convection is taken into account by means of an eddy viscosity flow model, which can represent the mixing effect of flow oscillations on the heat transfer.

Müller et al. [24,25] measured oxygen concentration within the melt volume using an electrochemical oxygen sensor. The oxygen sensor consists of thermocouple, solid ionic sensor and electronic melt contact.

2.3. MHD flow model

The demand for a large surface area of silicon wafers has fueled the upgrade of the wafer diameter of fabrication system from 200 mm to 300 mm. The change from 200 mm to 300 mm results in a threefold increase in the melt size. The turbulent flows in the silicon melt in large furnaces were usually controlled by applying a magnetic field, resulting in magnetohydrodynamic (MHD) flows.

Vizman et al. [26] carried out three-dimensional time-dependent numerical simulations to predict the oscillatory convection in a silicon Czochralski melt under the influence of a cusp-magnetic field (40 mT). The finite volume code STHAMAS 3D was used. The experiments were carried out in a Czochralski puller using a crucible diameter of 360 mm and a Si ingot of 20 kg, and the crystal diameter was kept constant at 104 mm. It was shown that the increase of magnetic field intensity regularized the flow more in the outer region than that in the core one. Both simulation and experiment have shown in correlation that large temperature fluctuations exist at the points under the crystal even at a maximum magnetic field intensity of 40 mT.

Liu et al. [27,28] proposed a novel model for three-dimensional (3D) global simulation in the silicon growth with a transverse magnetic field. This model overcomes the shortcoming of two- dimensional (2D) or 2D / 3D global model. It has been successfully used to predict the melt–crystal interface shape and the axial temperature gradients in solid and liquid near the interface [29]. Three-dimensional analysis of oxygen transport was carried out in silicon melts in a Czochralski growth process [30].

Chen et al. [31] developed a generalized, integrated model for complex crystal growth processes for semiconductor application that can be used to design and test these processes, and the numerical simulation was based on the second-order curvilinear finite volume discretization for fluid flow and transport phenomena (FLUTRAPP).

The dimensionless parameters Grashof number Gr, Marangoni number Ma, Prandtl number Pr, Hartmann number Ha, and rotational Reynolds numbers of the crystal and the crucible are as follows:

$$\begin{aligned} Gr &= g\beta b^3(T_w - T_m)/v^2 \\ Ma &= \frac{\partial\sigma}{\partial T}(T_w - T_m)b/(\rho v\alpha) \\ Pr &= v/\alpha, Ha = Bb\sqrt{\xi/\mu} \\ Re_s &= \omega_s b^2/v, Re_c = \omega_c b^2/v \end{aligned} \tag{1}$$

where g is the gravitational acceleration, β the thermal expansion coefficient, b the crucible radius, T_w the maximum temperature on the crucible wall, T_m the melting point of silicon, v the kinematic viscosity, $\frac{\partial\sigma}{\partial T}$ the surface tension differentiation with respect to temperature, α the thermal diffusivity, B the magnetic induction, ξ the electrical conductivity, ω_s the angular velocity of the crystal, and ω_c the angular velocity of the crucible.

Assuming that the Boussinesq's approximation can be applied to the buoyancy effect in the melt and that the flow is incompressible and Newtonian, the dimensionless governing equations are as follows:

$$\frac{\partial\bar\rho}{\partial t} + \frac{1}{r}\frac{\partial}{\partial r}(r\bar\rho u) + \frac{\partial}{\partial z}(\bar\rho w) = 0 \tag{2}$$

$$\begin{aligned} &\tfrac{\partial}{\partial t}(\bar\rho u) + \tfrac{1}{r}\tfrac{\partial}{\partial r}(r\bar\rho uu) + \tfrac{\partial}{\partial z}(\bar\rho wu) \\ &= \bar\mu\left[\tfrac{1}{r}\tfrac{\partial}{\partial r}\left(r\tfrac{\partial u}{\partial r}\right) + \tfrac{\partial^2 u}{\partial z^2} - \tfrac{u}{r^2}\right] - \tfrac{\partial p}{\partial r} + \bar\rho\tfrac{v^2}{r} + F_r \end{aligned} \tag{3}$$

$$\begin{aligned} &\tfrac{\partial}{\partial t}(\bar\rho v) + \tfrac{1}{r}\tfrac{\partial}{\partial r}(r\bar\rho uv) + \tfrac{\partial}{\partial z}(\bar\rho wv) \\ &= \bar\mu\left[\tfrac{1}{r}\tfrac{\partial}{\partial r}\left(r\tfrac{\partial v}{\partial r}\right) + \tfrac{\partial^2 v}{\partial z^2} - \tfrac{v}{r^2}\right] - \bar\rho\tfrac{uv}{r} + F_\theta \end{aligned} \tag{4}$$

$$\begin{aligned} &\tfrac{\partial}{\partial t}(\bar\rho w) + \tfrac{1}{r}\tfrac{\partial}{\partial r}(r\bar\rho uw) + \tfrac{\partial}{\partial z}(\bar\rho ww) \\ &= \bar\mu\left[\tfrac{1}{r}\tfrac{\partial}{\partial r}\left(r\tfrac{\partial w}{\partial r}\right) + \tfrac{\partial^2 w}{\partial z^2}\right] - \tfrac{\partial p}{\partial z} + Gr\Theta + F_z \end{aligned} \tag{5}$$

$$\begin{aligned} &R_C\left[\tfrac{\partial}{\partial t}(\bar\rho\Theta) + \tfrac{1}{r}\tfrac{\partial}{\partial r}(r\bar\rho u\Theta) + \tfrac{\partial}{\partial z}(\bar\rho w\Theta)\right] \\ &\quad = \tfrac{\bar k}{Pr}\left[\tfrac{1}{r}\tfrac{\partial}{\partial r}\left(r\tfrac{\partial\Theta}{\partial r}\right) + \tfrac{\partial^2\Theta}{\partial z^2}\right] \end{aligned} \tag{6}$$

where u, v and w are the dimensionless velocities in r, θ and z directions, respectively. The dimensionless density, viscosity, conductivity and heat capacity are $\bar\rho = \rho/\rho_l$, $\bar\mu = \mu/\mu_l$, $\bar k = k/k_l$, $R_C = C_p/C_{pl}$, respectively, where the subscript l denotes the liquid phase of silicon; the dimensionless temperature is $\Theta = (T - T_m)/(T_w - T_m)$; F is the Lorentz force.

A generalized equation for φ that represents Eqs. (2)–(6) is written as:

$$\frac{\partial\gamma\phi}{\partial t} + (\gamma\boldsymbol{u}\cdot\nabla)\phi = \nabla\cdot\Gamma\nabla\phi + S \tag{7}$$

where S is the source term including the body forces, pressure gradients and heat source. The energy balance at the interface is written as:

$$\rho_s h_{sl}(U_P(t)\boldsymbol{e}_z\cdot\boldsymbol{n} - \boldsymbol{U}_{int}\cdot\boldsymbol{n}) = -k_s\frac{\partial T}{\partial n} + k_l\frac{\partial T}{\partial n} \tag{8}$$

where $\boldsymbol{n}$ is the unit normal vector, $\mathbf{e}_z$ is the unit vector in the z direction, $\mathbf{U}_{int}$ is the velocity of interface movement, and

$U_P(t)$ is the pulling rate. At the free surface, the stress balance equation is

$$\boldsymbol{S}\cdot\boldsymbol{n} = -p_\infty \boldsymbol{n} + 2\sigma\chi\boldsymbol{n} + \frac{\partial\sigma}{\partial a}\boldsymbol{t} \tag{9}$$

where σ is the surface tension coefficient, χ is the mean curvature, a is the arc length, and $\boldsymbol{t}$ is the unit tangential vector.

By employing the classical solution of magnetic field for a single current loop, the magnetic field for a cusp magnetic-field configuration was calculated for the 200 mm silicon growth with a radius of crucible $b = 0.24$ m. The magnetic field was assumed to be unaffected by the fluid motions. After the magnetic field is obtained, the Lorentz force can be obtained.

Fig. 4 indicates the melt motions in the 200 mm Cz silicon single crystal furnace [31] when the crystal rotation speed is 15 rpm and the crucible rotation speed is -2 rpm. The dimensionless parameters are $Pr = 0.018$, $Gr = 1.15 \times 10^9$, $Ma = 1.12 \times 10^4$, and $Ha = 20$ corresponding to $B = 0.002$ T. The applied magnetic field for the 200 mm industrial growth is up to 0.04–0.12 T.

The high temperatures on the crucible wall result in buoyancy-driven flows in the melt because the Grashof number in this case is very high. Due to the crystal rotation, the fluid under the triple point (crystal/melt/gas) is pumped radially outwards, competing with the inward flow caused by the melt surface tension. A boundary layer is formed adjacent to the melt/crystal interface known as Ekmon boundary layer. This layer to some extent shields the interface from the vagaries of melt flow, thus helping in maintaining uniformity of the interface which is important from the crystal quality point of view. The solid/melt interface is concave towards the crystal. When the melt is sucked towards the crystal, it also brings the heat to the crystal, causing the bending of the temperature contours towards the crystal.

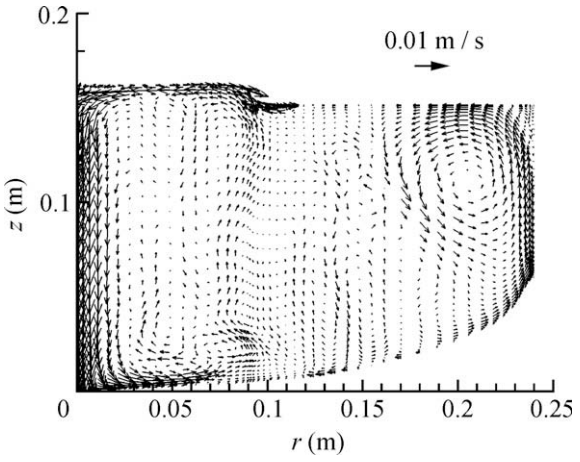

Fig. 4. Velocity field in the silicon melt in a 200 mm silicon growth system [31]. The rotation speeds are 15 rpm for crystal and −2 rpm for crucible.

2.4. Modeling of microgravity crystal growth

The thermocapillary flows have been simulated by many researchers. Peng et al. [32] performed unsteady three-dimensional simulations of thermocapillary-buoyancy flow of 0.65 cSt silicone oil (Prandtl number of 6.7) in annular pools with different depths (1 mm–11 mm). The annular pools were assumed to be heated from the outer wall and cooled at the inner cylinder, and with an adiabatic solid bottom and adiabatic free surface. In the shadow thin pool (depth of 1 mm), the hydrothermal wave characterized by curved spokes is dominant. In the deep pools (depth of 5 mm or more), the three-dimensional stationary flow appears and the flow pattern corresponds to the Rayleigh-Bénard instability, which consists of pairs of counter-rotating longitudinal rolls. When the depth is between 1 mm and 5 mm, the hydrothermal wave and the three-dimensional oscillatory flow coexist in the pool and travel along the same azimuthal direction with the same angular velocity.

Friedrich et al. [33] performed global thermal modeling of germanium crystal growth that was carried out in the low gradient furnace (LGF) in the Materials Science Laboratory (MSL) onboard the International Space Station (ISS). For a given translation velocity of the cartridge in the LGF, the temperature field and shape of the solid–liquid interface were calculated.

3. Ammonothermal growth modeling

3.1. Model development

Models of the hydrothermal/ammonothermal growth have been developed in the last 10 years since Chen et al. [34,35] performed the 3-D flow modeling in a hydrothermal growth system using a porous media flow model based on the Darcy-Brinkman-Forchheimer formulation. For the ammonothermal growth, aqueous ammonia is used as a solvent while water is used in the hydrothermal growth.

Chen et al. [36] modeled ammonothermal systems using fluid dynamics, thermodynamics and heat transfer models, and studied the effects of particle size on flow pattern and temperature distribution in the autoclave. Ammonothermal growth was developed in the 1990s by Dwilinski et al. [5], who obtained microcrystals of BN, AlN and GaN using lithium or potassium amide as mineralizer at pressures in the range of 1–5 kbar and temperatures up to 550 °C. The ammonothermal growth of 1-inch size (0001) GaN crystal in a cylindrical high-pressure autoclave with an internal diameter of 40 mm was reported by Hashimoto et al. [37]. The applied temperature and pressure were 625–675 °C and about 2.14 kbar, respectively. Basic mineralizers were used to have a retrograde solubility of GaN in supercritical ammonobasic solutions. The nutrient was placed in the colder region (upper region) and free-standing c-plane HVPE-GaN seed crystals were placed in the hotter region (lower region). A baffle divided the

reactor into an upper region and a lower region to set a temperature difference between the dissolving region and the crystallization region. Uniform growth of GaN films on an over-1-in. oval-shaped seed crystal was achieved through fluid transport of Ga nutrient.

Kashiwagi et al. [38] studied the nitrogen transfer from the surface of the flux to the interface in the LPE growth of GaN with a solution of Na and Ga using a global model that considers radiative, convective and conductive heat and mass transfer. They obtained the growth rate of the GaN epitaxial layer. Growth rate of the GaN epitaxial layer is limited by mass transfer in the flux in the LPE system. Control of the convection of the flux is a key issue for controlling growth rate of the epitaxial layer of GaN by the LPE technique.

3.2. Porous media flow

Chen et al. [39] modeled the GaN growth process in an autoclave with an internal diameter of 2.22 cm, external diameter of 7.62 cm, internal height of 35.56 cm and external height of 45.72 cm (Tem-Press MRA 378R with a volume of 134 ml). The Grashof number is estimated to be 4.46×10^6 based on the inner radius of the autoclave. Fig. 5 shows the fluid flow in an autoclave with a baffle opening of 20% in the cross-sectional area, e.g. 10% in the central hole and 10% in the ring opening between the baffle and the sidewall of autoclave [39]. The flow goes up in the ring opening between the baffle and the sidewall of autoclave and comes back in the central opening causing strong mixing of fluid across the baffle. The flow in the porous layer is very weak, and the flow in the fluid layer is much stronger. The modified Grashof number, which is the product of the Grashof number and Darcy number, can be used to measure the flow strength in the porous charge. Here, the modified Grashof number is $Gr^* = Gr \cdot Da = 228$. Thus, heat and mass transfer in the porous layer is caused mainly by conduction and diffusion. This will constrain the nutrient transport between the charge and fluid layer, and cause nutrient deposition on the sidewall of the autoclave near the fluid/charge interface as observed in experiments.

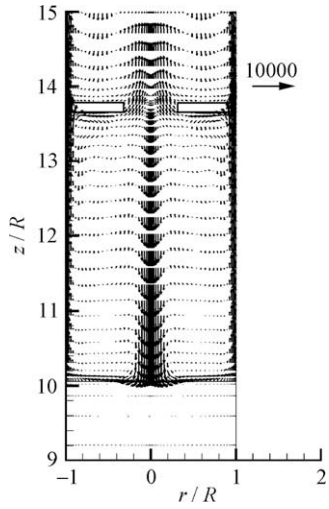

Fig. 5. Fluid flow in a system with a baffle opening of 20% in the cross-sectional area (central opening of 10% and ring opening of 10%) [39].

4. Modeling of PVT growth

4.1. Conduction-radiation model

Modeling and simulation of SiC crystal growth has attracted significant research attention in the last 10 years or so, and many growth models have been developed such as those proposed by Hofmann et al. [40,41], Pons et al. [42,43], Egorov et al. [44], Müller et al. [45,46], Karpov et al. [47], Ma et al. [48], Chen et al. [49–53], Selder et al. [54], Räback et al. [55–57], and Chen et al. [58]. Various degrees of system complexity have been considered in these models, e.g. the electromagnetic field produced by RF heating, heat power generated in the graphite susceptor, conduction and radiation heat transfer, and the growth kinetics.

Hofmann et al. [40,41] developed a numerical process model based on a finite volume scheme FASTEST to simulate the heat transfer in a 2-inch SiC growth set-up, and obtained the flow field in the growth chamber caused by the buoyancy effect. The growth temperature was estimated to be 2573 K and the system pressure was up to 3500 Pa. Pons et al. [42,43] used a finite element code Flux-Expert to calculate the electromagnetic field and temperature distribution and found that the predicted temperatures for the seed and powder surface (2920 K and 3020 K) are much larger than the external temperatures measured at the top and the bottom of the crucible (2390 K and 2500 K), while the maximum temperature of the insulation foam on its periphery is about 1000 K. The total pressure is around 4000 Pa and the growth rate is 1.55 mm/h. Egorov et al. [44] modeled the global heat transfer inside the system for SiC growth in a tantalum container. Müller et al. [45,46] calculated the temperature distributions in inductively heated SiC growth reactors in temperatures of 2373-2673 K, and found that the temperatures in the powder are highly non-uniform. They predicted that the radial variations were 30-50 K along the powder surface. Karpov et al. [47] calculated the growth rate in the growth of SiC in a tantalum container.

Ma et al. [48] performed an order-of-magnitude analysis of parameters in the SiC PVT growth, and used a one-dimensional network model and a two-dimensional finite-volume model to predict the temperature distribution in a 75 mm growth system. The 1-D flow-kinetics model for the PVT growth of SiC was proposed by Chen et al. [49], which assumes that the growth rate is proportional to the supersaturation of SiC species near the growth interface, and the transport of SiC vapor species is through both the Fickian diffusion and Stefan flow. Chen et al. [50–53] investigated the effects of temperature, temperature

gradient and inert gas pressure on the growth rate, and obtained the growth rate profile across the seed surface from the temperature distribution in a 75 mm growth system. The powder charge is modeled as a solid matrix with a porosity and an effective conductivity that accounts for both the conduction and radiation in the powder.

Selder et al. [54] introduced a modeling approach to the simulation of heat and mass transfer during SiC bulk crystal growth and compared the calculated results with the experimental data. Räback et al. [55–57] presented a model for the growth rate of SiC sublimation process and estimated the parametric dependencies of the growth rate.

Chen et al. [58] used the global model to optimize the design of a crucible for a SiC sublimation growth. They calculated the induction heating, temperature field and growth rate for a sublimation growth system of silicon carbide and found that the thickness of the substrate holder, distance between the powder and substrate, and angle between the crucible wall and powder free surface were important for both growth rate and crystal quality.

4.2. Stepan flow model

Chen et al. [59] proposed a 2-D flow-kinetics theory for the vapor growth, and obtained the concentration distribution and flow field inside the crucible. The SiC growth system considered has five turns of RF coil. By using an induction frequency of 8 kHz and a current of 1400 A in the induction coil, the seed temperature was calculated to be 2671 K, and the charge temperature was calculated to be 2691 K. The concentration distribution of the combined species Si_2C and Si was assumed to be the same as that of SiC_2. The molar fluxes caused by diffusion are around 10.1 times as much as that by convection at the center of the seed for the argon pressure of 8 kPa. The mass transfer in the growth cavity is dominated by diffusion. The concentration at the charge, which remains the highest in the field, is almost two times as much as that near the seed. There is a positive concentration gradient on the seed surface, and this is caused by the positive temperature gradient along the seed surface.

The flow field corresponding to the growth pressure of 8 kPa was obtained [59] (Fig. 6), and the growth rate was estimated to be 0.8 mm/h in this case. The velocity profile on the charge surface is not uniform due to the non-uniform temperature distribution, and a high velocity corresponds to a high local temperature. The radial velocity distribution at the seed depends strongly on the growth kinetics, and a high velocity corresponds to a low local temperature. The high velocity induced by a low temperature at the center of the seed causes a faster growth rate than that near the edge of the seed, resulting in a convex shape of the crystal. The velocity on the side wall of the crucible is zero.

Desirable growth temperature and inert gas pressure were obtained to achieve certain growth rate profile across the seed surface. The enlargement of the bulk crystal was realized by designing a system with a large radial temperature gradient at the beginning of the growth process. The SiC growth modeling has helped in improving the growth processes and in designing larger diameter growth systems.

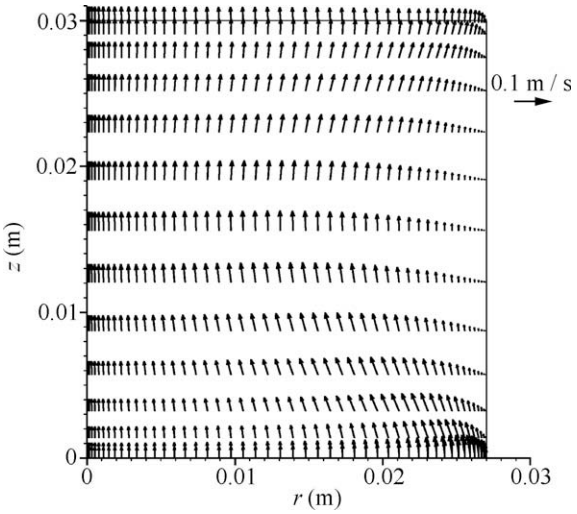

Fig. 6. Flow field in the growth chamber at the growth pressure of 8 kPa [59].

5. Conclusions and perspectives

The complexity of crystal growth is a formidable challenge to computer modeling due to the very small spatio-temporal scales, as well as the frequent occurrence of non-laminar flows. The only way to obtain vital information about growth mechanisms is through in-situ observation of growth processes using X-ray radiography [21], synchrotron and neutron scattering facilities [60].

Modeling has emerged as an important tool for design and development of crystal growth processes. Using numerical models, extensive parametric studies can be performed to optimize the growth conditions and study the effects of changes in geometric configurations. Global models can greatly help in the design of new systems as well as in the modifications in the existing equipment. Due to diversity of materials and processes involved in the growth processes, modeling requires multidisciplinary approaches and different numerical methods. The trends of research in the modeling of crystal growth processes are listed as follows.

5.1. Multiscale modeling

With the increasing computational power, the modeling of multiscale problems in crystal growth processes is becoming possible. The crystal growth processes take place on very different spatio-temporal scales. The temporal scales for the defect formation and dislocation movement in a growing crystal are usually smaller than those for the variations of the fluid field and thermal field. The

spatial scales for the formation of dendrites, grains and facets are smaller than those of the furnace.

5.2. Coupling of 2D and 3D modes

For the global modeling of temperature within the furnace in the Czochralski growth of silicon and the ammonothermal growth of GaN, it is completely sufficient and efficient to use an axisymmetric model. However, the flows are highly turbulent, requiring three-dimensional model for fluid flows. The convective processes within the melt and the solution have a significant influence on the growth of the crystals. The coupling of a global axisymmetric temperature model with a detailed three-dimensional flow model is desirable.

5.3. Flow-kinetics model for vapor growth

The vapor growth of silicon carbide is relevant to the Stefan flow, which is caused by the volumetric expansion of the solid into the gas phase. The flow-kinetics theory for the vapor growth can be used to explain the growth mechanism of SiC and to predict the growth rates at different growth conditions.

5.4. Parallelisation

Due to the generally high temperatures in the crystal growth processes, heat transfer by radiation plays a dominant role. The radiation in the vapor growth can be modeled satisfactorily using the view-factor method if the diffuse reflection can be assumed. However, for optical crystals, 3D model for volumetric radiations is required. The computation of view factors and 3D simulation of flows can be parallelized.

Acknowledgment

This work was supported by the National Natural Science Foundation of China (Grant Nos. 10432060 and 50776098).

References

[1] Lan CW. Recent progress of crystal growth modeling and growth control. Chem Eng Sci 2004;59:1437–57.
[2] Byrappa K, Yoshimura M. Handbook of hydrothermal technology. New York: William Andrew Publishing; 2001.
[3] Chen QS, Prasad V, Zhang H. Et al. Silicon carbide crystals - Part II: Process physics and modeling. In: Crystal growth technology. NY: William Andrew; 2003, 233–269.
[4] Czochralski J. A new method for the measurement of crystallization rate of metals. Zeitschrift für physikalische Chemie 1918;92:219–21 (in German).
[5] Dwilinski R, Doradzinski R, Garczynski J, et al. Ammono method of BN, AlN and GaN synthesis and crystal growth. MRS Internet J. Nitride Semicond Res 1998;3(25):1–4.
[6] Tairov YM, Tsvetkov VF. Investigation of growth processes of ingots of silicon carbide single crystals. J Cryst Growth 1978;43:209–12.
[7] Derby JJ, Brown RA. Thermal-capillary model of Czochralski and liquid-encapsulated Czochralski crystal growth: 1. Steady-state simulation. J Cryst Growth 1986;74:605–24.
[8] Derby JJ, Brown RA. Thermal-capillary analysis of Czochralski and liquid encapsulated Czochralski crystal growth. J Cryst Growth 1986;75:227–40.
[9] Brown RA, Kinney TA, Sackinger PA, et al. Toward an integrated analysis of Czochralski growth. J Cryst Growth 1989;97:99–115.
[10] Bornside DE, Kinney TA, Brown RA. Finite-element/Newton method for analysis of Czochralski crystal growth with diffuse-gray radiation. Inter J Numer Meth Engng 1990;30:133–54.
[11] Kinney TA, Brown RA. Application of turbulence modeling to integrated hydrodynamic thermal-capillary model of Czochralski crystal growth of silicon. J Cryst Growth 1993;132:551–74.
[12] Lipchin A, Brown RA. Comparison of three turbulence models for simulation of melt convection in Czochralski crystal growth of silicon. J Cryst Growth 1999;205(1–2):71–91.
[13] Lipchin A, Brown RA. Hybrid finite-volume/finite-element simulation of heat transfer and turbulence in Czochralski crystal growth of silicon. J Cryst Growth 2000;216:192–203.
[14] Jafri IH, Prasad V, Anselmo AP, et al. Role of crucible partition in improving Czochralski melt conditions. J Cryst Growth 1995;154:280–92.
[15] Zhang H, Prasad V. A multizone adaptive process model for low and high-pressure crystal growth. J Cryst Growth 1995;155:47–65.
[16] Chui WK, Glimm J, Tangerman FM, et al. A parallel algorithm for multizone, multiphase systems with application to crystal growth. J Cryst Growth 1997;180(3–4):534–42.
[17] Zhang H, Zheng LL, Prasad V, et al. Diameter-controlled Czochralski growth of silicon crystals. J Heat Transfer 1998;120:874–82.
[18] Zhang T, Wang GX, Zhang H, et al. Turbulent transport of oxygen in the Czochralski growth of large silicon crystals. J Cryst Growth 1999;198:141–6.
[19] Nunes EM, Naraghi MHN. Numerical model for radiative heat transfer analysis in arbitrarily shaped axisymmetric enclosures with gaseous media. Numer Heat Transfer Part A 1998;33:495–513.
[20] Gevelber MA. Dynamics and control of the Czochralski process. IV. Control structure design for interface shape control and performance evaluation. J Cryst Growth 1994;139:286–301.
[21] Kakimoto K, Eguchi M, Watanabe H, et al. Flow instability of molten silicon in the Czochralski configuration. J Cryst Growth 1990;102:16–20.
[22] Kakimoto K, Nicodeme P, Lecomte M, et al. Numerical simulation of molten silicon flow–comparison with experiment. J Cryst Growth 1991;114(4):715–25.
[23] Assaker R, VandenBogaert N, Dupret F. Time-dependent simulation of the growth of large silicon crystals by the Czochralski technique using a turbulent model for melt. J Cryst Growth 1997;180(3–4):450–60.
[24] Seidl A, Marten R, Müller G. Oxygen distribution in Czochralski silicon melts measured by an electrochemical oxygen sensor. Mater Sci Eng B 1996;36:46–9.
[25] Müller G, Mühe A, Backofen R, et al. Study of Oxygen transport in Cz growth of silicon. Microelectron Eng 1999;1:135–47.
[26] Vizman D, Gräbner O, Müller G. 3D numerical simulation and experimental investigations of melt flow in a Si Czochralski melt under the influence of a cusp-magnetic field. J Cryst Growth 2002;236(4):545–50.
[27] Liu LJ, Kakimoto K. Partly three-dimensional global modeling of a silicon Czochralski furnace. I. Principles, formulation and implementation of the model. Int J Heat Mass Transfer 2005;48:4481–91.
[28] Liu LJ, Kakimoto K. Partly three-dimensional global modeling of a silicon Czochralski furnace. Model application: Analysis of a silicon Czochralski furnace in a transverse magnetic field. Int J Heat Mass Transfer 2005;48:4492–7.
[29] Liu LJ, Nakano S, Kakimoto K. An analysis of temperature distribution near the melt–crystal interface in silicon Czochralski growth with a transverse magneticfield. J Cryst Growth 2005;282:49–59.

[30] Liu LJ, Nakano S, Kakimoto K. Investigation of oxygen distribution in electromagnetic Cz-Si melts with a transverse magnetic field using 3D global modeling. J Cryst Growth 2007;299:48–58.
[31] Chen QS, Deng GY, Ebadian A, et al. Numerical study on flow field and temperature distribution in growth process of 200 mm Czochralski silicon crystals. J Rare Earths 2007;25:345–8.
[32] Peng L, Li YR, Shi WY, et al. Three-dimensional thermocapillary–buoyancy flow of silicone oil in a differentially heated annular pool. Int J Heat Mass Transfer 2007;50:872–80.
[33] Friedrich J, Dagner J, Hainke M, et al. Numerical modeling of crystal growth and solidification experiments carried out under microgravity conditions. Cryst Res Technol 2003;38:726–33.
[34] Chen QS, Prasad V, Chatterjee A. Modeling of fluid flow and heat transfer in a hydrothermal crystal growth system: use of fluid-superposed porous layer theory. J Heat Transfer 1999;121:1049–58.
[35] Chen QS, Prasad V, Chatterjee A, et al. A porous media-based transport model for hydrothermal growth. J Cryst Growth 1999;198/199:710–5.
[36] Chen QS, Prasad V, Hu WR. Modeling of ammonothermal growth of nitrides. J Cryst Growth 2003;258:181–7.
[37] Hashimoto T, Fujito K, Saito M, et al. Ammonothermal growth of GaN on an over-1-inch seed crystal. Jpn J Appl Phys 2005;44:1570–2.
[38] Kashiwagi D, Gejo R, Kangawa Y, et al. Global analysis of GaN growth using a solution technique. J Cryst Growth 2008;310(7–):1790–3.
[39] Chen QS, Pendurti S, Prasad V. Effects of baffle design on fluid flow and heat transfer in ammonothermal growth system of nitrides. J Cryst Growth 2004;266(1–3):271–7.
[40] Hofmann D, Heinze M, Winnacker A, et al. On the sublimation growth of SiC bulk crystals: development of a numerical process model. J Cryst Growth 1995;146:214–9.
[41] Hofmann D, Eckstein R, Kölbl M, et al. SiC-Bulk Growth by Physical-Vapor Transport and its Global Modelling. J Cryst Growth 1997;174:669–74.
[42] Pons M, Blanquet E, Dedulle JM, et al. Thermodynamic heat transfer and mass transport modeling of the sublimation growth of silicon carbide crystals. J Electrochem Soc 1996;143(11):3727–35.
[43] Pons M, Blanquet E, Dedulle JM, et al. Different macroscopic approaches to the modeling of the sublimation growth of SiC single crystals. Mater Sci Eng B 1997;46:308–12.
[44] Egorov YE, Galyukov AO, Gurevich SG, et al. Modeling analysis of temperature field and species transport inside the system for sublimation growth of SiC in tantalum container. Mater Sci Forum 1998;264–268:61–4.
[45] Müller SG, Eckstein R, Hofmann D, et al. Modelling of the PVT-SiC bulk growth process taking into account global heat transfer, mass transport and heat of crystallization and results on its experimental verification. Mater Sci Forum 1998;264–268:57–60.
[46] Müller SG, Glass RC, Hobgood HM, et al. The status of SiC bulk growth from an industrial point of view. J Cryst Growth 2000;211:325–32.
[47] Karpov SY, Kulik AV, Zhmakin IA, et al. Analysis of sublimation growth of bulk SiC crystals in tantalum container. J Cryst Growth 2000;211:347–51.
[48] Ma RH, Chen QS, Zhang H, et al. Modeling of silicon carbide crystal growth by physical vapor transport method. J Cryst Growth 2000;211:352–9.
[49] Chen QS, Zhang H, Prasad V, et al. Kinetics and modeling of sublimation growth of silicon carbide bulk crystals. J Cryst Growth 2001;224(1–2):101–10.
[50] Chen QS, Zhang H, Ma RH, et al. Modeling of transport processes and kinetics of silicon carbide bulk growth. J Cryst Growth 2001;225(2–4):299–306.
[51] Chen QS, Zhang H, Prasad V, et al. Modeling of heat transfer and kinetics of physical vapor transport growth of silicon carbide crystals. J Heat Transfer –Transactions of ASME 2001;123:1098–109.
[52] Prasad V, Chen QS, Zhang H. A process model for silicon carbide growth by physical vapor transport. J Cryst Growth 2001;229(1–):510–5.
[53] Chen QS, Zhang H, Prasad V. Heat transfer and kinetics of bulk growth of silicon carbide. J Cryst Growth 2001;230(1–2):239–46.
[54] Selder M, Kadinski L, Makarov Y, et al. Global numerical simulation of heat and mass transfer for SiC bulk crystal growth by PVT. J Cryst Growth 2000;211:333–8.
[55] Räback P, Nieminen R, Yakimova R, et al. A coupled finite element model for the sublimation growth of SiC. Mater Sci Forum 1998;264–268:65–8.
[56] Räback P, Yakimova R, Syväjärvi M, et al. A practical model for estimating the growth rate in sublimation growth of SiC. Mater Sci Eng B 1999;61–62:89–92.
[57] Räback P. Modeling of the sublimation growth of silicon carbide crystals. Doctoral dissertation, Helsinki University of Technology, Espoo, Finland, 1999.
[58] Chen XJ, Liu LJ, Tezukab H, et al. Optimization of the design of a crucible for a SiC sublimation growth system using a global model. J Cryst Growth 2008;310:1810–4.
[59] Chen QS, Yan JY, Prasad V. Application of flow-kinetics model to the PVT growth of SiC crystals. J Cryst Growth 2007;303:357–61.
[60] Boatner L, Beasley M, Canfield P, et al. Design, discovery and growth of novel materials for basic *research*: an urgent U.S. need, Report on the DOE/BES workshop: ''Future Directions of Design, Discovery and Growth of Single Crystals for Basic Research'', Ames laboratory, Iowa State University, 2003.